31st Congress of the International Council of the Aeronautical Sciences

Belo Horizonte, Brazil; September 09-14, 2018

GLOBAL SENSITIVITY ANALYSIS OF TRANSONIC FLUTTER USING A COUPLED CFD-CSD SOLVER

Rimple Sandhu*, Weixing Yuan, Dominique Poirel*****
*** Carleton University and Visiting Scholar at National Research Council, Ottawa, Canada**
**** National Research Council (NRC) Canada, Ottawa, Canada**
***** Royal Military College (RMC) of Canada, Kingston, Canada**

Keywords: *Aeroelasticity, sensitivity analysis, computational fluid dynamics (CFD), computational structural dynamics (CSD), fluid-structure interaction (FSI)*

Abstract

Transonic aeroelastic flutter analysis is performed using time-domain simulations of three-dimensional (3D) aircraft wings through partitioned coupling of a computational fluid dynamics (CFD) solver and a computational structural dynamics (CSD) solver. In particular, the AGARD standard configuration 'Wing 445.6' and the associated experimental data are considered to validate and verify the coupled CFD-CSD solver. Upon validation, the nonlinear transonic aeroelastic behaviour, specifically the effects of under-wing store properties on transonic flutter is investigated using global sensitivity analysis in conjunction with the validated coupled CFD-CSD Solver.

1 Introduction

Flutter is a dangerous unstable oscillation encountered in flexible structures subjected to aerodynamic forces. Commercial and military aircraft (such as Canada's CF-18 fighter jets) often operate at a speed close to the speed of sound (transonic speed). At transonic speeds, shock-wave-induced nonlinear aerodynamics produces a dip (drop) in the flutter boundary thereby limiting the flight envelope and undermining the safe operation of the aircraft [1]. When the flight speed is above the flutter boundary, the aircraft will experience flutter phenomena. Up until recently, linearized aerodynamic theories have been used for flutter certification. However, transonic flutter is inherently nonlinear. In the Canadian context, a nonlinear aeroelasticity prediction capability is being developed where the nonlinear fluid-structure interaction (FSI) system is simulated using a high-fidelity algorithm that couples the solutions from computational fluid dynamics (CFD) and computational structural dynamics (CSD) solvers [2].

In this work, an integrated CFD-CSD approach is developed and validated for the simulation and prediction of flutter. The CFD solver was developed by the German Aerospace Research Center (DLR), based on an unsteady, parallel, multi-block, multi-grid, structured, finite volume algorithm for the Euler/Navier-Stokes equations [3]. The flowfield solution is coupled with the structural dynamics by a fully implicit method. A 3D CSD solver using a finite element model based on linear elasticity equations are employed for high-fidelity simulations. The coupled CFD-CSD method simulates the elastic system directly in the time domain to determine the stability of the aeroelastic system.

Despite the use of highly sophisticated computational tools to predict flutter, there remains significant uncertainty in whether flutter will occur at a particular condition because of the high sensitivity of the flutter phenomenon to small variations or uncertainties in operating conditions, under-wing store (e.g., missile, rocket, fuel tank, etc.) configurations, material behaviour, and numerical modelling assumptions. Moreover, modern aircraft tend to possess a high level of flexibility to satisfy maneuverability requirements resulting in the need to perform thorough investigations of potential instabilities in the presence of variations in flight parameters. In this work, an uncertainty quantifi-

cation (UQ) and sensitivity analysis (SA) framework is developed to comprehend the propagation of such uncertainties through the high-fidelity CFD-CSD simulations and to identify their effects on the FSI dynamics, in particular the transonic flutter phenomenon. The probabilistic UQ/SA framework will treat the uncertain parameters as random variables with a known probability distribution governed by operational demands, inherent variability, or lack of knowledge. SA is performed through global sensitivity analyses (GSA) procedures wherein sensitivity measures will help identify inputs as important or redundant with respect to a quantity-of-interest (QOI). This reduction in the number of salient parameters leads to a more informed and targeted use of resources for tasks such as design of experiments and design optimization. UQ/SA framework also enables inclusive understanding of critical phenomena such as transonic flutter, thereby ensuring safer operation of flight at transonic speeds.

Currently, the Canadian establishment does not have expertise in the area of UQ/SA for FSI systems. Even in the public domain, only limited literature exists on explicit consideration of parametric uncertainties and their influence on the flight envelope. Pettit [4] provided a comprehensive review of UQ applications in aeroelasticity and how UQ complements advances in deterministic computational mechanics of FSI systems. Janardhan et al. [5] studied the effect of certain store configurations on the flutter dynamics, albeit qualitatively and only for certain specific store properties. In this work, we treat the input parameters as random variables wherein entire range of values are considered for computing UQ/SA entities. Computing SA importance measures through push-forward of random input samples from high-fidelity FSI code is rendered impractical due to high computational cost of the time-domain FSI simulations. In this work, we augment the UQ/SA framework with a surrogate building procedure that provides the UQ/SA entities as a by-product and requires minimum simulation runs of the FSI code. Sudret [6] stated that the polynomial chaos expansion (PCE) surrogate is known to provide the best choice for executing UQ/SA with minimum input-output samples.

The long-term goal of this study is to apply the UQ/SA framework as a risk analysis tool to aerospace applications. The intermediate objective is to build a robust and efficient UQ/SA framework powered through a surrogate model, and to establish a proof-of-concept with its application to transonic aeroelasticity and flutter analysis.

In this work we consider the 'weakened model 3' of the AGARD 445.6 wing from Yates [7] as a test bed to validate and verify the coupled CFD-CSD code and the subsequent UQ/SA framework. The transonic flutter predictions from this wing configuration will be compared against available experimental data to thoroughly validate the high-fidelity FSI algorithm followed by UQ/SA investigations on the effect of certain store properties on the flutter speed index in transonic regime. This wing configuration will be referred to as 'the wing' when discussed together with under-wing configurations, unless stated otherwise.

In Section 2 we discuss the details of the coupled CFD-CSD solver designed for the AGARD 445.6 wing. In Section 3, we discuss the details of GSA procedures and the associated surrogate building approach. In Section 4 we compare the results from the CFD-CSD code with that from the experiments, followed by SA results pertaining to under-wing store properties.

2 Coupled CFD-CSD solver for FSI

2.1 CSD Model

The CSD model for the AGARD 445.6 wing comprises of a 3D finite element model satisfying linear elasticity equations which were built using Elmer FEM software package [8]. The wing has a 2.5-foot semi span, and consists of a symmetric NACA 65A004 airfoil, a sweep angle of 45° and a taper ratio of 0.66. The wing geometry was modelled as a rectangular cross-section 3D beam with planform dimensions (chord length, span, swept) the same as that of the wing. The wing geometry was meshed using second-order 3D tetrahedron elements generated using GMSH software [9]. The material proper-

ties of the wing published in Yates [7] were adjusted to better align the first four modal frequencies with experimental values. The modal frequencies (Table 1) and mode shapes (Figure 1) for the CSD model of AGARD 445.6 wing were obtained using Eigen analysis. Although the calculated frequencies were not identical to the measured ones, which needs to be refined, they were in a reasonable agreement with the published values [7] and that of the plate model (details not included in this paper). The time-domain CSD model was obtained by discretizing the time-varying elasticity equations in a fully implicit manner using Bossak method [10]. The free-decay time-history of the trailing edge at wing tip and its frequency content is shown in Figure 2. The frequency content of the time-history is in agreement with the modal frequencies.

2.2 CFD Model

The CFD solver employed was the German DLR FLOWer code [3]**.** This Navier-Stokes solver uses a block-structured computational domain around the aerodynamic configuration. The flow equations were discretized based on the finite-volume approach. A cell-centred formulation was used for the discretization. Convective fluxes were evaluated by using a second-order accurate central differencing scheme with scalar dissipation, according to Jameson et al. [11]. Alternatively, the advection upstream splitting method (AUSM), similar in principle to the van Leer flux vector splitting scheme [12], is available [13], which was employed for transonic flow simulations in this study. For time-accurate calculations, an implicit time integration according to the dual time-stepping approach was employed. Convergence was accelerated by the use of multigrid. The turbulence transport equations were computed separately from the Reynolds-averaged Navier-Stokes (RANS) equations on a single-grid basis at the finest grid level. A first-order accurate flux-difference upwind scheme, according to Roe [14], was used for the convective fluxes of the turbulence equations, and a fully implicit integration scheme was employed for the temporal discretization. Most of the standard turbulence models (algebraic eddy-viscosity models, one- and two-equation models, algebraic stress and Reynolds stress models) are available. The Menter SST model [15] was considered for the unsteady RANS (URANS) calculations presented in this study.

The calculations were performed on moving grid configurations. The velocity of the grid movement was included in the governing equations in an inertial frame of reference. In order to avoid artificial mass sources generated by the grid velocity, a space conservation law was introduced to ensure a fully conservative property in the computations. The geometric conservation law was discretized in time, which relates the discrete displacement and the discrete mesh velocity, and thus ensures the numerical accuracy.

2.3 CFD-CSD Coupling

In the partitioned fluid-structure interaction system, the grid of the discretized aerodynamic model is usually placed on the external surface, whereas the structural model is placed on the internal load-carrying component. These require the proper data transfer between the two computational grid systems, which amounts to the proper transfer of the displacement computed in the structural grid to the aerodynamic grid and that of the loads from the aerodynamic grid to the structural grid. This process requires significant attention to detail. Similar to the aeroelastic analysis software ZAERO [16], we used the spline matrices that relate or interpolate the displacements at the structural finite element grid points to aerodynamic points.

The CFD and CSD codes were fully coupled. In order to obtain a stable and accurate solution with a partitioned scheme, pseudo-time stepping (sub-iterations) was used. The CFD and CSD solvers exchanged information after each pseudo-time step.

3 Theory: Global Sensitivity Analysis

Sensitivity analyses [17] [18] are a set of numerical procedures aimed at understanding the uncertainty composition of the outputs of a model, given the uncertainties in the inputs to

the model. SA is purely a data-driven approach that treats the system model as a black-box, and only the input-output samples are used to assign a sensitivity index or an importance measure to each input or set of inputs. The importance measure serves as an indicator of the influence of each input in the uncertainty in the model output. SA methods can be categorized into: 1) local SA, 2) screening methods, and 3) global SA. Global SA is the preferred way to perform sensitivity studies as the importance measures are computed using a representative sample set from the entire input domain (unlike local SA). GSA treats variance as a proxy for the uncertainty, whereby the output variance is decomposed into contributions by individual model inputs or their interactions.

Consider that the input-output relation is denoted as $Y = f(X_1, X_2, .., X_d)$ where Y is the model output (flutter speed index), f (.) is the system model (coupled CFD-CSD code), and X_i is the i-th input (store mass, store location etc.). In this work, the probability distribution for the input parameters X_i (under-wing store characteristics) is assumed to be known from the operational requirements of the associated aircraft. The uncertainty in the input parameter is pushed-forward through the FSI model f (.), resulting in the uncertainty in the output Y. Through GSA we aim to quantify the contribution of each X_i in the variance of Y.

GSA operates by quantifying the sensitivity in terms of two importance measures: 1) First-order sensitivity index, and 2) Total-order sensitivity index. The first-order index quantifies the effect of each input on output uncertainty occurring without any interaction with other inputs. The total-order sensitivity index quantifies the effect of each input including the effect due to its interaction with other inputs. The total-order also includes the first-order effect and so total-order index is always greater than the corresponding first-order index. Also, if the sum of all first-order indices adds to 1 then the input-output relation is linear wherein there are no interactions (nonlinearity) in the model, and the . 47, No. 2, pp 135fully decomposed into contributions due to individual inputs. In this work, we will use GSA to quantify the sensitivity of flutter speed to the store properties.

Saltelli [19] proposed a computational algorithm for computing first-order and total-order sensitivity indices using Monte Carlo (MC) samples from input probability distribution. However, computing sensitivity indices through push-forward of input MC samples through the high-fidelity FSI code is rendered computationally expensive. In this work, we seek to estimate the GSA sensitivity indices through a polynomial chaos expansion (PCE) surrogate of the input-output relation. Building PCE surrogate requires much less FSI model runs as compared to direct computation of sensitivity indices using MC samples. Once PCE surrogate is available, sensitivity indices are readily available without any additional computational effort. In this work, we will use Clenshaw-Curtis (CC) quadrature points to estimate the PCE coefficients through non-intrusive spectral projection [6]. The CC quadrature is a nested technique, meaning quadrature points from the subsequent levels includes the points from previous levels, thereby enabling the check on accuracy of PCE surrogate constructions without any additional computational effort.

4 Numerical Results

4.1 Validation of Coupled CFD-CSD Solver

The coupled CFD-CSD code was validated using the weakened model 3 of the AGARD 445.6 wing from Yates [7]. A non-dimensional entity called speed index, $V = U_\infty / (b_s \omega_\theta \sqrt{\mu})$, is used to gauge the flutter prediction capabilities of various FSI models. Note that U_∞ is the freestream velocity, b_s is the streamwise semi-chord at the wing root, μ is the wing panel mass ratio and V_f is the speed index at flutter.

Figure 3 shows the damped, neutral, and divergent responses, respectively for Mach = 0.901. The flutter speed index was computed by observing the amplitude change in the time history of deflections and aerodynamic coefficients. As evidenced by Table 2, the comparison of the computed flutter speed index for Mach = 0.901 with the experimental and numerical results published in Yates [7] shows a reasonable agreement. The transonic regime is par-

ticularly interesting due to the shock-wave induced aerodynamic nonlinearities resulting in a sudden drop in flutter speed index. Figure 4 further illustrates the comparison of flutter speed index obtained using the coupled CFD-CSD code with that from Yates [7] in the transonic region. The computed results also compare reasonably well with the theoretical and experimental data from other researchers [7].

4.2 Sensitivity of Flutter Speed to Under-wing Store Properties

We performed a sensitivity study on the effect of under-wing store properties on transonic flutter, using the validated CFD-CSD solver for the AGARD 445.6 wing at Mach = 0.901. For this purpose, we augmented the wing geometry with a pylon/store attachment, as shown in Figure 5. The pylon/store attachment was meshed using 3D solid tetrahedron elements and thus modelled using linear elasticity equations, similar to the wing. For simplicity at this stage, the pylon/store attachment was not included in the aerodynamic simulations and hence the CFD-CSD interface remains unchanged from that of the pure wing simulations. Note that even though the aerodynamic loads on the pylon/store attachment were not considered, the deflection of the store attachment affects the wing dynamics which in turn affects the aerodynamics. Also note that the aerodynamic shape of the pylon/store was irrelevant in this study and the centre of gravity (CG) for the pylon and store coincided in span-wise and chord-wise directions.

For the sake of sensitivity study we chose the following store properties and their associated probability distributions:

- Pylon/store CG distance (positive towards trailing edge) from mid-chord at mid-span, $X_s \sim$ Uniform (-0.15,0.15) m
- Store mass, $M_s \sim$ Uniform (0.5,1.5) kg

Note that Mach = 0.901 was held fixed in the transonic regime along with other CFD-CSD model parameters. Also, the store CG location along the span was fixed at the midspan. In order to isolate the effect of store mass and to enable the coupling of store modes with wing modes, we assumed that the pylon was massless but highly flexible (low Young's modulus). The store was assumed to be rigid (high Young's modulus). The range of values considered for store mass and CG location were inspired from a scaled version of Canada's CF-18 fighter aircraft. For example, the range of store mass (0.5-1.5 kg) is assumed to be approximately between 25%-100% of the wing mass (1.83 kg). The variation in store CG location was derived from ever-changing operational requirements of modern fighter aircraft.

Next, we performed CFD-CSD model runs at nine quadrature points generated using Clenshaw-Curtis quadrature method for different combinations of store mass and CG location, as shown in Figure 6. The flutter speed index was computed for each quadrature point using the coupled CFD-CSD simulations. As demonstrated in Figure 3, it needed multiple runs to narrow down the speed index to the flutter condition by monitoring the growth of amplitude for deflections and aerodynamic coefficients.

Comparing the time-histories of deflections and aerodynamic coefficients for the same flow parameters but varying store properties provides an interesting qualitative preview of sensitivity analysis results. For example, Figure 7 compares the time-histories for varying store CG location but fixed store mass (1.0 kg). As mentioned earlier, the store was located at the mid-span. It is realized that both flutter speed and flutter frequency decreased (amplitude diverging more rapidly) as the store CG moved towards the trailing edge. Note that the decrease was more pronounced when the store CG moved from mid-chord to trailing edge than it was from leading edge to mid-chord. Figure 8 compares the time history for varying store mass but fixed store CG location at the trailing edge. It is realized that the severity of amplitude divergence increased with the store mass and hence the flutter speed index decreased with increase in store mass. Also, the flutter frequency decreased with increasing store mass. Note that this decrease in flutter speed index and flutter frequency with increasing store mass was not so severe when the store CG was at mid-chord (results not shown here). These qualitative obser-

vations made by varying one parameter and fixing others motivated us to pursue GSA, providing a robust qualitative sensitivity analysis framework that incorporates the effect due to interaction between varying parameters. GSA eliminates the need for visual inspection by quantifying the sensitivities in terms of first-order and total-order sensitivity indices.

To compute GSA sensitivity indices, a PCE surrogate was built using the input quadrature points (X_s and M_s) and the corresponding output (V_f) obtained using the CFD-CSD simulations. The PCE coefficients are estimated using non-intrusive spectral projection approach. Figure 9 shows the probability density function (PDF) for the input (store mass and CG location) and the output (flutter speed index) obtained using PCE surrogate. Even though the store mass and CG location were uniformly distributed, the flutter speed index had a non-trivial distribution and was more skewed towards the higher end. This distribution of the flutter speed index further motivates the application of probabilistic and inclusive UQ/SA methods to understand the effect of operational variabilities on aircraft aerodynamics.

Table 3 lists the GSA sensitivity indices obtained using the PCE surrogate. Higher first-order index for store CG location indicates a higher influence of store CG location over store mass. In fact, a value of 0.655 for first-order index implies that the 65.5% of variance in flutter speed index was produced by the variation in store CG location. The addition of first-order indices is 0.913, meaning 8.7% of the variance in flutter speed index was due to interaction between store mass and CG location. This observation is crucial for flutter store clearance as one cannot overlook store CG location in chordwise direction when deciding appropriate store mass.

Finally, Figure 10 shows the projected flutter speed index variation obtained using PCE surrogate within the entire input domain. Such plots can act as input to the store clearance process and/or in the design of aircraft wings/pylons. Note that the accuracy of projected flutter speed values in Figure 10 is conditioned on the goodness of PCE surrogate, which we have no way to confirm or deny due to limited input-output sample set.

5 Concluding Remarks

A coupled CFD-CSD code was developed and validated using a benchmark case of the AGARD 445.6 wing against the associated experimental data. A probabilistic PCE surrogate powered UQ/SA framework was developed to ascertain the influence of under-wing store properties on transonic flutter. A numerical study concerning the effect of store mass and CG location on flutter speed index was undertaken to establish a proof-of-concept for the application of UQ/SA framework to high-fidelity FSI models in a computationally feasible fashion.

6 Acknowledgments

The authors gratefully acknowledge the support of the Department of National Defence of Canada (DND) through the DTAES' AERAC program. Prof. Abhijit Sarkar at the Carleton University has participated in the project concept design and provided valuable advices for the code development and algorithm implementation. The CFD code FLOWer was provided by the German Aerospace Center (DLR), Institute of Aerodynamics and Flow Technology. Jochen Raddatz at DLR has provided valuable suggestions and discussions regarding the use of the FLOWer CFD code.

References

[1] Bendiksen, O. Review of Unsteady Transonic Aerodynamics: Theory and applications. *Aerospace Sciences*, Vol. 47, No. 2, pp 135-167, 2011.

[2] Yuan, W., Sandhu, R., De Matos, O., Poirel, D. Methodology Development for Coupled Aeroelastic Analysis of Wing Flutter. *54th AIAA Aerospace Sciences Meeting*, AIAA 2016-1550, 2016.

[3] Kroll, N. and Fassbender, J. K. MEGAFLOW – Numerical Flow Simulation for Aircraft Design. *Notes on Numerical Fluid Mechanics and Multidisciplinary Design*, Vol. 89, Springer Verlag, Berlin, 2005.

[4] Pettit, C.L. Uncertainty Quantification in Aeroelasticity: Recent Results and Research Challenges. *Journal of Aircraft*, Vol. 41, No. 5, pp 1217-1229, 2004.

[5] Janardhan, S., Grandhi, R.V., Eastep, F., Sanders, B. Parametric Studies of Transonic Aeroelastic Effects of an Aircraft Wing/tip Store. *Journal of Aircraft*, Vol. 42, No. 1, pp. 253-263, 2005.

[6] Sudret, B. Global Sensitivity Analysis using Polynomial Chaos Expansions. *Reliability Engineering & System Safety*, Vol. 93, No. 7, pp 964-979, 2008.

[7] Yates, E. *AGARD Standard Aeroelastic Configurations for Dynamic Response, Candidate Configuration I.-Wing 445.*6. Technical Memorandum 100492, NASA, 1987.

[8] http://www.elmerfem.org.

[9] Geuzaine, C. and Remacle, J.-F. GMSH: A Three-dimensional Finite Element Mesh Generator with Built-in Pre- and Post-processing Facilities. *International Journal for Numerical Methods in Engineering*, Vol. 79, No. 11, pp 1309-1331, 2009.

[10] Wood, W.L., Bossak, M., and Zienkiewicz, O.C. An Alpha Modification of Newmark's Method. *Int. J. Num. Meth. Eng*., Vol, 15, pp 1562-1566, 1981.

[11] Jameson, A., Schmidt, W., and Turkel, E. Numerical Solutions of the Euler Equations by Finite Volume Methods using Runge-Kutta Time-Stepping Schemes. AIAA Paper 81-1259, 1981.

[12] Van Leer, B. Towards the Ultimate Conservative Difference Scheme. V. A Second-Order Sequel to Godunov's Method. *Journal of Computational Physics*, Vol. 32, pp 101-136, 1979.

[13] Kroll, N. and Radespiel, R. *An Improved Flux Vector Split Discretization Scheme for Viscous Flows*, DLR-FB 93-53, Institute of Aerodynamics and Flow Technology, German Aerospace Center, 1993.

[14] Roe, P. L. Approximate Riemann Solvers, Parameter Vectors and Difference Schemes. *Journal of Computational Physics*, Vol. 43, pp 357-372, 1981.

[15] Menter, F.R. Two-Equation Eddy-Viscosity Transport Turbulence Model for Engineering Applications. *AIAA Journal*, Vol. 32, pp 1598-1605, 1994.

[16] ZONA Technology, Inc. *Zaero Theoretical Manual, Engineers' Tool Kit for Aeroelastic Solutions*. 2011.

[17] Homma, T., and Saltelli, A. Importance Measures in Global Sensitivity Analysis of Nonlinear Models. *Reliability Engineering and System Safety*, Vol. 52, No. 1, pp 1-17, 1996.

[18] Sobol, I.M. Sensitivity Estimates for Nonlinear Mathematical Models. *Mathematical Modeling and Computational Experiment*, Vol. 1, No. 4, pp 407-414, 1993.

[19] Saltelli, A. Making Best Use of Model Evaluations to Compute Sensitivity Indices. *Computer Physics Communications*, Vol. 145, No. 2, pp 280-297, 2002.

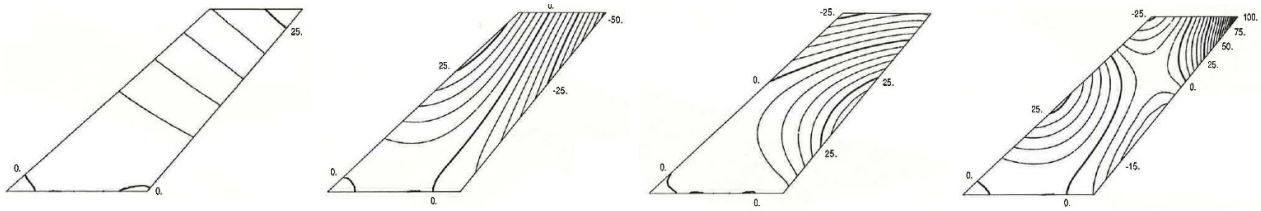

Mode 1, $f = 9.6$ | Mode 2, $f = 38.17$ | Mode 3, $f = 48.35$ | Mode 4, $f = 91.54$

Adopted from Yates

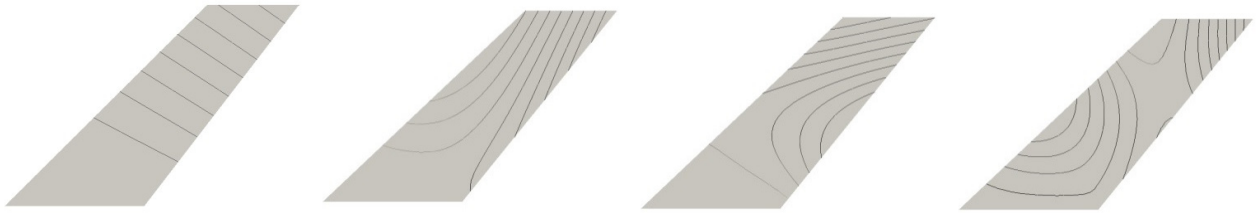

Mode 1, $f = 10.00$ | Mode 2, $f = 37.60$ | Mode 3, $f = 53.35$ | Mode 4, $f = 91.74$

3D FEM

Figure 1. First four mode shapes for the 'Weakened model 3' of the AGARD 445.6 wing.

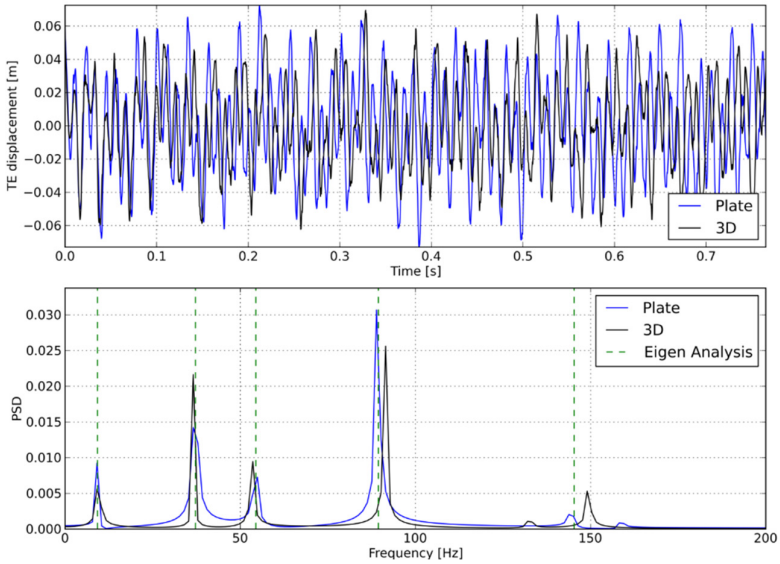

Figure 2. Time marching solution of wing tip by ignoring aerodynamic forcing.

$V = 0.300$

$V = V_f \approx 0.331$

$V = 0.364$

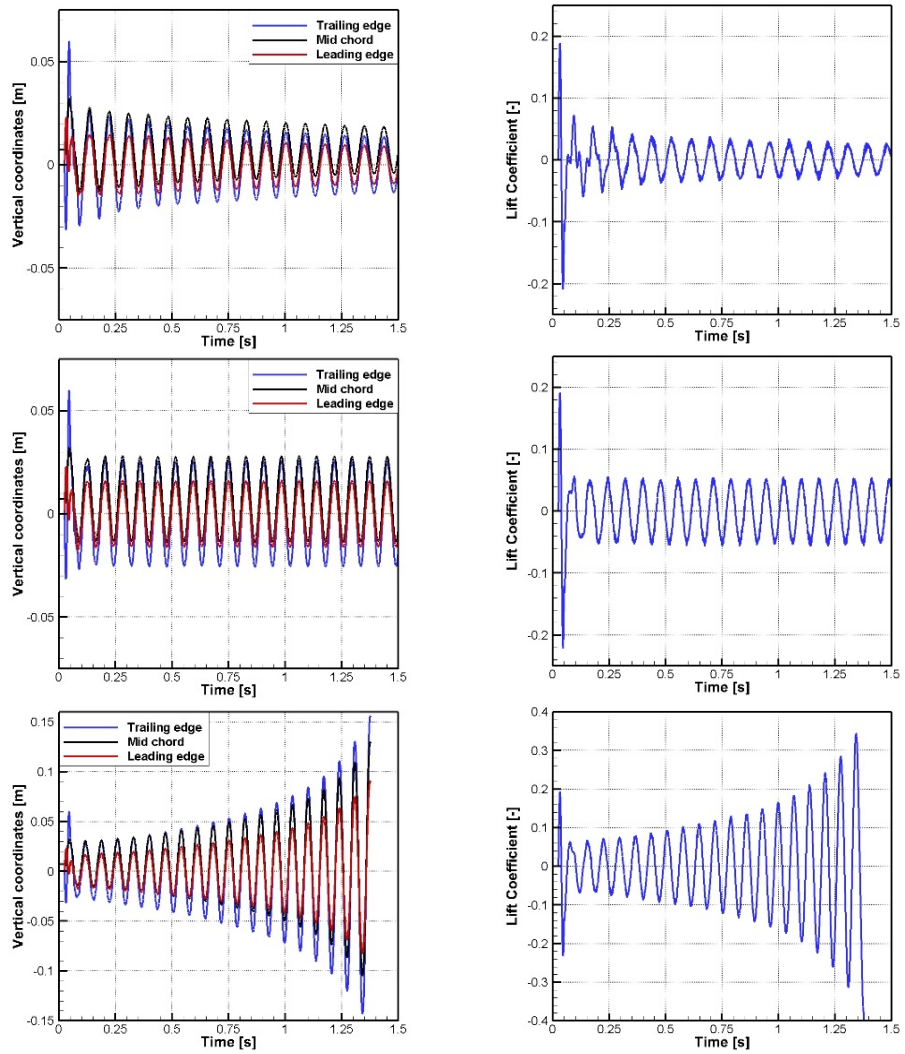

Figure 3. Computed time history of deflections and lift coefficients for the AGARD 445.6 wing for $M_\infty = 0.901$.

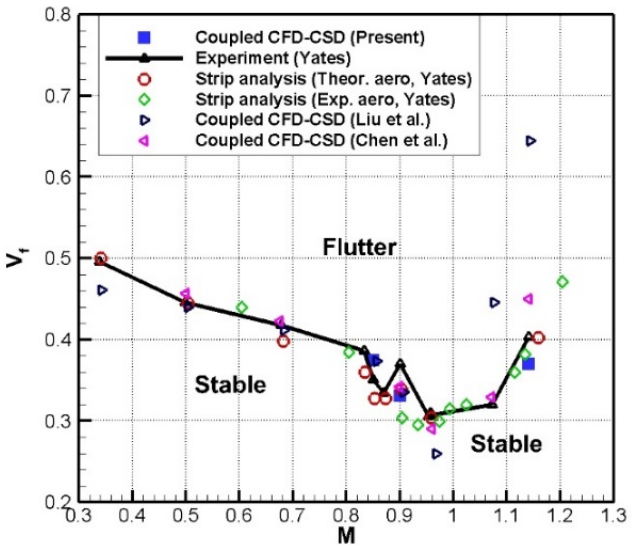

Figure 4. Comparisons of flutter boundary for the AGARD 445.6 wing.

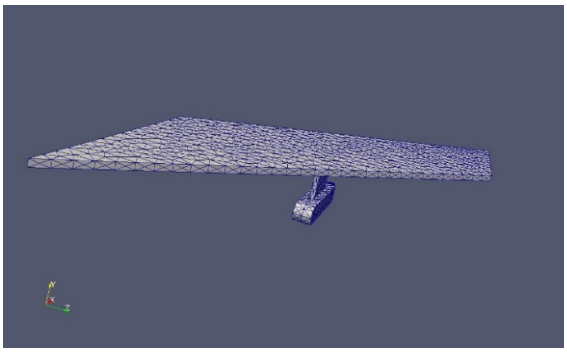

Figure 5. Wing and pylon/store 3D structural model (Store located a mid-span).

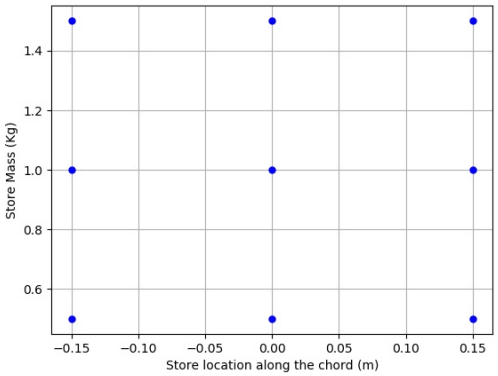

Figure 6. Clenshaw-Curtis (CC) quadrature to estimate PCE coefficients and GSA sensitivity indices.

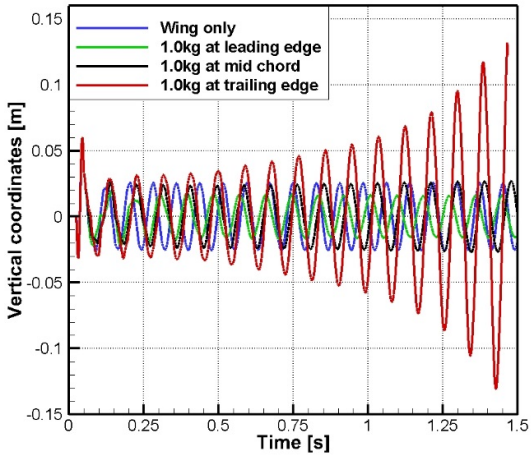

Figure 7. Time history of deflection for different store location along the chord.

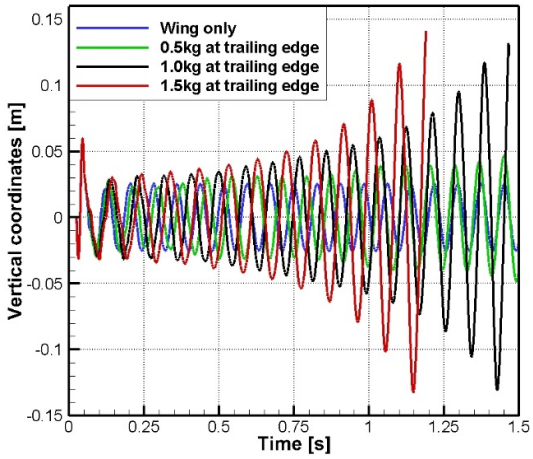

Figure 8. Time history of deflection for different store mass.

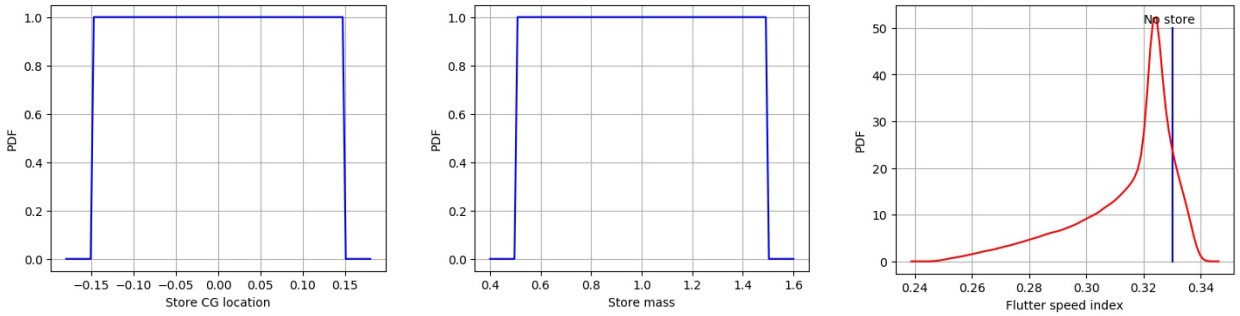

Figure 9. Input and output probability density functions.

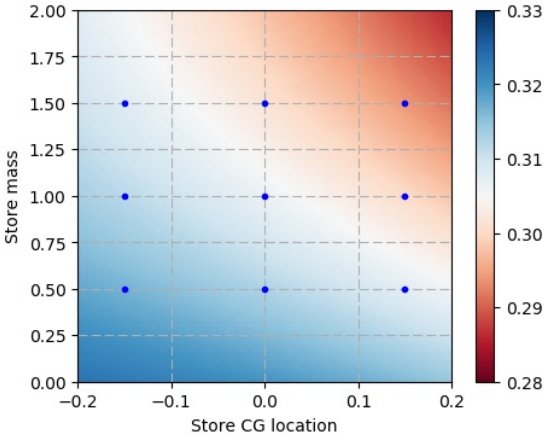

Figure 10. Projected flutter speed indices using PCE surrogate (within the input domain). Note: pure wing V_f= 0.3309.

Table 1 Eigenvalue analysis for the 'Weakened model 3' of the AGARD 445.6 wing

	Experimental [7]	Numerical [7]	Plate model	3D model
Mode 1 (Hz)	9.60	9.60	8.72	10.00
Mode 2 (Hz)	38.10	38.17	39.04	37.60
Mode 3 (Hz)	50.70	48.35	58.07	53.35
Mode 4 (Hz)	98.50	91.45	101.8	91.74

Table 2 Comparisons of flutter boundary for the AGARD 445.6 wing at M = 0.901

Experimental [7]	Strip Analysis - Theo. Aero. [7]	Strip Analysis - Meas. Aero. [7]	3D model
0.3700	0.3385	0.3038	0.331

Table 3 Global sensitivity results for flutter speed index

Parameter	First-order SI	Total-order SI	Interaction effects
Store location, X_s	0.655	0.742	0.087
Store Mass, M_s	0.258	0.345	

Copyright Statement